Published in final edited form as:
Neuroscience. 2012 October 25; 223: 365–376. doi:10.1016/j.neuroscience.2012.07.053.

Adenosine Receptor Activation Is Responsible for Prolonged Depression Of Synaptic Transmission After Spreading Depolarization in Brain Slices

Britta E. Lindquist and **C. William Shuttleworth**
Department of Neurosciences, University of New Mexico School of Medicine, 1 University of New Mexico, Albuquerque NM 87131, USA, BLindquist@salud.unm.edu; BShuttleworth@salud.unm.edu

Abstract

Spreading depolarization (SD) is a slowly propagating, coordinated depolarization of brain tissue, which is followed by a transient (5–10 min) depression of synaptic activity. The mechanisms for synaptic depression after SD are incompletely understood. We examined the relative contributions of action potential failure and adenosine receptor activation to the suppression of evoked synaptic activity in murine brain slices. Focal micro-injection of KCl was used to induce SD and synaptic potentials were evoked by electrical stimulation of Schaffer collateral inputs to hippocampal area CA1. SD was accompanied by loss of both presynaptic action potentials (as assessed from fiber volleys) and field excitatory postsynaptic potentials (fEPSPs). Fiber volleys recovered rapidly upon neutralization of the extracellular DC potential, whereas fEPSPs underwent a secondary suppression phase lasting several minutes. Paired-pulse ratio was elevated during the secondary suppression period, consistent with a presynaptic mechanism of synaptic depression. A transient increase in extracellular adenosine concentration was detected during the period of secondary suppression. Antagonists of adenosine A1 receptors (DPCPX or 8-CPT) greatly accelerated fEPSP recovery and abolished increases in paired-pulse ratio normally observed after SD. The duration of fEPSP suppression was correlated with both the duration of the DC shift and the area of tissue depolarized, consistent with the model that adenosine accumulates in proportion to the metabolic burden of SD. These results suggest that in brain slices, the duration of the DC shift approximately defined the period of action potential failure, but the secondary depression of evoked responses was in large part due to endogenous adenosine accumulation after SD.

Keywords

Adenosine; A1 receptors; DC shift; spreading depression; voltage-inactivation; CA1

INTRODUCTION

Spreading depolarization (SD) is a coordinated wave of neuronal and glial depolarization that propagates slowly through brain tissue at ~2–5 mm/min, driven by the feed-forward

Corresponding Author: C. William Shuttleworth, Department of Neurosciences, University of New Mexico School of Medicine, 1 University of New Mexico, Albuquerque NM 87131, USA, Ph: 505 272 4290, Fax: 505 272 8082, Bshuttleworth@salud.unm.edu.

release of glutamate and/or K^+ into the extracellular space. During SD, massive and prolonged Na^+ and Ca^{2+} inward currents are accompanied by a large negative shift in the extracellular direct current (DC) potential (Somjen, 2001, Dreier, 2011). Recovery from the large ionic disturbances resulting from SD is metabolically demanding and depletes tissue ATP and glycogen levels (Shinohara et al., 1979, Mies and Paschen, 1984, Selman et al., 2004). Repetitive SDs in compromised tissue have been strongly implicated in the progression of acute brain injury in animal models (Back et al., 1996, Hartings et al., 2003) and more recently, SD has been observed with high incidence in clinical recordings. In the injured brain, SDs with long DC shift durations have been associated with poor clinical outcomes (Dreier et al., 2009, Hartings et al., 2011b). Understanding SD and its consequences could be of significant benefit for the treatment of migraine, traumatic brain injury, ischemic stroke, and subarachnoid hemorrhage (Dreier, 2011, Lauritzen et al., 2011).

The classical consequence of spreading depolarization is a profound and relatively long-lasting (many minutes) suppression of both spontaneous and evoked synaptic activity, first described as spreading depression of cortical activity (Leao, 1944, see Bures et al., 1974, Somjen, 2001). Longlasting, reversible depression of evoked synaptic activity is also observed in isolated brain slice preparations (e.g. Jing et al., 1991, Wu and Fisher, 2000, Wernsmann et al., 2006). The mechanisms responsible for the depression of synaptic activity after SD have not been resolved. One likely contributor is failure of action potential propagation, as SD involves collapse of electrochemical gradients required for cation entry and causes prolonged depolarization sufficient to inactivate voltage-gated sodium channels (depolarization block) (see Kager et al., 2000, and discussion in Dreier et al., 2012). However, the duration of synaptic depression is typically much longer (up to ~10 min) than elevation of extracellular potassium or cellular depolarization during SD, which usually conclude in the order of ~ 1 min (Somjen and Giacchino, 1985, Somjen et al., 1990). Thus it is likely that other mechanisms, in addition to disrupted ionic gradients and voltage-dependent inactivation of ion channels, are involved in the prolonged suppression of synaptic activity.

Previous work suggests extracellular adenosine as a candidate mediator of prolonged synaptic depression following SD. A low energy metabolite of ATP, adenosine accumulates in the settings of decreased metabolic supply (hypoxia, ischemia) or increased metabolic demand from coordinated neuronal activation (Fowler, 1989, Mitchell et al., 1993, Dunwiddie and Masino, 2001). Activation of G-protein coupled adenosine A1 receptors (A1Rs) can depress synaptic transmission through pre- and postsynaptic mechanisms (Thompson et al., 1992, and reviewed in Dunwiddie and Masino, 2001). Adenosine increases have been detected during SD in rat hippocampus *in vivo* (Kaku et al., 1994). A gradual accumulation of adenosine and A1R-dependent suppression of synaptic transmission has been reported during oxygen and glucose deprivation (OGD) in brain slices, which is then followed by larger increases during the onset of anoxic depolarization (AD) (Frenguelli et al., 2007). A1R-dependent synaptic depression also develops rapidly during glial-selective inhibition of oxidative metabolism with fluoroacetate, and protects neuronal viability by delaying SD (Canals et al., 2008). While adenosine accumulation during OGD or fluoroacetate exposure can be partly explained by the inhibition of metabolism prior to SD-like events, this prior work suggests that spreading depolarization itself may induce adenosine accumulation. However it has not yet been explicitly tested whether a burst of adenosine accumulation and activation of A1 receptors might contribute to suppression of synaptic activity when SD is generated without prior inhibition of metabolism.

Here, we utilized a well-validated brain slice model to evaluate the relative contributions of depolarization block and adenosine accumulation to the transient depression of synaptic transmission after SD. SD was generated by microinjection of KCl and confirmed with both

optical and electrophysiological methods. The findings indicate that depolarization block is limited to the period of the DC shift, and that A1R activation by endogenous adenosine mediates a significant portion of the suppression of evoked synaptic transmission following SD. Preliminary findings of these studies have been presented in abstract form (Lindquist and Shuttleworth, 2011).

EXPERIMENTAL PROCEDURES

Animals and slice preparation

All procedures using animals were performed in accordance with protocols approved by the UNM Health Sciences Center Institutional Animal Care and Use Committee. C57Bl/6 mice at 4–10 weeks of age were used for all studies. Slice preparation was as previously described (Shuttleworth et al., 2003). Briefly, animals were deeply anesthetized with a mixture of ketamine and xylazine, decapitated, and brains were removed into oxygenated ice-cold cutting solution. Brains were hemisected and cut in the coronal orientation (350 μm slices) with a Pelco 102 Vibratome (Ted Pella, Inc., Redding, CA). Immediately after cutting, slices were incubated at 35°C for 60 min in artificial cerebrospinal fluid (aCSF) then cooled to room temperature, for holding until transfer to the recording chamber.

Electrophysiology

Individual brain slices were transferred to a submersion recording chamber with nylon slice supports (RC-27, Warner Instruments, Hamden CT), and continuously superfused with aCSF (2 ml/min), maintained at 34°C by an inline heater assembly (TC-344B, Warner Instruments). A concentric Pt/Ir bipolar stimulating electrode (FHC, Bowdoin ME) driven by a current controller with direct current (DC) power supply (A.M.P.I, Jerusalem, Israel) was positioned in the stratum radiatum of CA1 for stimulation of Schaffer collateral inputs. Extracellular excitatory postsynaptic potentials (fEPSPs) were recorded with glass microelectrodes filled with aCSF (tip resistance 2–6 MΩ) and placed in the stratum radiatum, approximately 250 μm from the stimulation site and 30–50 μm below the slice surface (see Figure 1A). Responses were recorded at 10 kHz with an Axon MultiClamp 700B amplifier and Clampex 9.2 (Molecular Devices, Sunnyvale CA). Slices were equilibrated in the recording chamber for 15 minutes prior to recording and then an input-output curve was generated. Test pulses or pairs of pulses were then delivered (70 μs, 0.1 Hz) at intensities that gave 60–75% of maximum fEPSP responses (120–400 μA), and were below the threshold for generation of population spikes. The effects of drugs were also tested on a form of short-term synaptic plasticity termed paired pulse facilitation, generated by stimulating presynaptic fibers at a short interpulse interval (50ms). At such short intervals, enhancement of the amplitude of the second evoked potential occurs, and has been attributed to enhanced presynaptic release probability, as assessed from quantal analysis (see Thomson, 2000, Zucker and Regehr, 2002). In the current study, this degree of facilitation was quantified as paired pulse ratio (PPR), calculated from the peak amplitudes of ($amplitude_{fEPSP2}$/$amplitude_{fEPSP1}$), after excluding evoked responses with amplitudes less than 1.5× baseline noise.

SD was induced only after a stable fEPSP baseline was established. SD was induced by microinjecting KCl (1 M) through a glass micropipette (2–6 MΩ) placed in the stratum radiatum approximately 250 μm from the bipolar electrode (pressure pulse (40–200 ms, 60 psi) delivered by a WPI PV830 Pneumatic Picopump (World Precision Instruments, Sarasota FL)).

Imaging

Slices were trans-illuminated with visible light (≥600 nm) and viewed with either 4× (Olympus 0.10 NA) or 10× (Olympus 0.30 NA) objectives. Images were captured with a cooled CCD camera (Imago VGA, TillPhotonics GmBH, Gräfelfing, Germany), and analyzed using TillVision software (TillPhotonics, version 4.01). Intrinsic optical signals (IOS) associated with SD have been described previously and peak sharply at the wave-front of SD, simultaneous with DC shifts (Andrew et al., 1999). IOS was normalized to baseline and expressed as percent change in transmission ($\Delta T/T_0 \times 100$). A slow second phase of increased light transmission was quantified by calculating the area under the curve ($\Delta T/T_0$ % × time). The extent of tissue involved in SD was determined from IOS recordings made at 4× magnification, by tracing the perimeter of the maximum IOS signal and calculating the enclosed area in ImageJ (version 1.46, National Institutes of Health, Bethesda, MD; see Figure 3B).

Adenosine measurements

Enzyme-coupled electrochemical probes sensitive to adenosine (SBS-ADO-05-50) were purchased from Sarissa Biomedical Ltd (Coventry, UK) and operated with a MicroC two-electrode DC potentiostat (World Precision Instruments, Sarasota FL). These biosensors incorporate adenosine deaminase, purine nucleoside phosphorylase, and xanthine oxidase to generate an amperometric signal proportional to concentrations of adenosine and inosine (see Dale and Frenguelli, 2012). Control studies with an inhibitor of adenosine deaminase (*erythro*-9-(2-hydroxy-3-nonyl)adenine hydrochloride, EHNA, 5 μM) verified the contribution of adenosine to measured signals (see Results). Calibrations followed guidelines from the manufacturer, and used a high concentration of adenosine (100 μM, Sigma Aldrich, St. Louis MO) in aCSF as a reference, given the large increases observed following SD. In our hands, electrode responses were linear in the 0–100 μM range. Adenosine references were measured in the recording chamber with tissues, alternately preceding or following SD studies. Complete washouts (>10 min) were maintained between measurements. While the entire surface area of the probe was accessible to the test solution, only a small portion of the probe was in contact with the brain slice, and therefore measurements of endogenous adenosine accumulation are likely to be systematically underestimated by this comparison with exogenous adenosine.

Drugs and Solutions

The aCSF contained (in mM): NaCl 126, $NaHCO_3$ 26, glucose 10, KCl 3, $CaCl_2$ 2, H_2PO_4 1.5, and $MgSO_4$ 1 and was equilibrated with 95% O_2 / 5% CO_2. Cutting solution contained (in mM) sucrose 220, $NaHCO_3$ 26, glucose 10, $MgSO_4$ 6, KCl 3, NaH_2PO_4 1.5, $CaCl_2$ 0.2, and was equilibrated with 95% O_2/ 5% CO_2 and supplemented with 0.2 ml ketamine (100 mg/ml, Putney Inc, Portland ME) per 100 ml cutting solution.

All salts and glucose for aCSF were obtained from Sigma-Aldrich Corporation (St. Louis MO). 6,7-Dinitroquinoxaline-2,3(1H,4H)-dione (DNQX, Sigma-Aldrich) was prepared as a stock in DMSO (50 mM) and diluted to a working concentration of 10 μM in aCSF. 8-Cyclopentyl-1,3-dipropylxanthine (DPCPX, Sigma Aldrich) and 4-(-2-[7-amino-2-(2-furyl)(1,2,4)triazolo(2,3-a)(1,3,5triazin-5-ylamino] ethyl)phenol (ZM 241385, Tocris Bioscience, Bristol, UK) were each prepared as 1 mM stock solutions in ethanol, and diluted to a final working concentration of 500nM in aCSF. Tubing was changed and the recording chamber was extensively washed between drug and vehicle trials, as DPCPX effects were observed to carry over to subsequent experiments if this precaution was omitted. Stock solutions of *erythro*-9-(2-Hydroxy-3-nonyl)adenine hydrochloride (EHNA, Tocris) 5 mM and 8-Cyclopentyl-1,3-dimethylxanthine (8-CPT, Sigma) 20 mM were prepared in DMSO;

Suramin (Sigma) 50 mM and N6-cyclopentyl adenosine (CPA, Sigma) 1 mM were dissolved in deionized water.

Analysis

Electrophysiology and electrochemistry signals were acquired in Clampex 9.2 and evaluated using Clampfit 9.2 (Molecular Devices, Sunnyvale CA). DC shifts and electrochemical currents were low-pass filtered (1 Hz cut-off). fEPSPs were resolved from continuous recordings with a high pass filter (1 Hz cut-off) and measured with Clampfit's Event Detection function. Durations of DC shifts were determined by measuring the time from maximum negative potential to 80% recovery (t_{80}). Recovery of fEPSP amplitude was measured as the time required for responses to first reach ≥50% of baseline values (t_{50}), and the duration of the DC shift or the duration of loss of fiber volley was subtracted to isolate the secondary phase of fEPSP suppression after SD.

Data are reported as mean ± SEM. Statistical analyses (analysis of variance (ANOVA), paired-and unpaired t-tests, Fisher's exact test, linear regression and correlation tests) were calculated using GraphPad Prism (version 5.04, La Jolla CA). Statistical significance was determined by p values <0.05, with Bonferroni correction in the case of multiple comparisons.

RESULTS

1. Two phases of synaptic transmission block after spreading depolarization

Spreading depolarization (SD) was evoked in the hippocampal CA1 region of brain slices by microinjection of KCl (≥500 μm distant from the recording electrode) and observed as a shift in DC potential and a propagating increase in intrinsic optical signal (IOS, see Experimental Procedures, Figure 1 A&B). To determine the relationship of SD to the generation of action potentials, presynaptic fiber volleys were recorded before, during, and after SD. Figure 1C shows responses to stimulation of Schaffer collateral inputs, (single pulses, 0.1 Hz) in the presence of the glutamate receptor antagonist DNQX (10 μM) to isolate fiber volleys. Complete block of fiber volleys was confirmed with tetrodotoxin (TTX, 1 μM, n=3). SD was readily induced in the presence of DNQX (DC shift amplitude −5.84±0.43 mV, duration 33.2±2.3 s, propagation rate 3.4±0.3 mm/min, n=7), consistent with previous observations (Muller and Somjen, 2000). Under these conditions, fiber volleys were completely abolished immediately following arrival of SD at the recording electrode and could not be evoked during the extracellular DC potential shift. As the DC potential recovered, the fiber volley recovered and was fully restored within 42.4±3.3 s after the peak negative DC potential (n=7).

In parallel studies without DNQX, fiber volleys could be reliably resolved from postsynaptic potentials. Under these conditions, a similar duration of fiber volley suppression was observed following SD (Figure 1D). As seen in DNQX, there was a close relationship between the duration of DC shifts and the absence of fiber volleys. In control conditions (aCSF containing 0.05% ethanol vehicle), the DC shift lasted 23.3±3.3 s (n=7), while in a separate group of recordings under the same conditions, the fiber volley was abolished for 28.3±3.1 s (n=6). As expected, postsynaptic potentials were never observed during fiber volley block. Thus in all cases, SD resulted in a short period of absolute, primary suppression of transmission.

Figure 2 shows the time course of normalized fiber volley and fEPSP amplitudes before, during, and after SD in a representative slice. The sequence of recovery of synaptic potentials seen following SD in the present study was in agreement with previous descriptions (Kawasaki et al., 1988). During SD, there was a complete suppression of both

the fiber volley and fEPSP ("b" in Figure 2). Immediately following recovery of the fiber volley, all slices (6/6 in this series) displayed a partial transient recovery of postsynaptic responses. Events at this time point ("c" in Figure 2) appeared to involve complex population spike activity, analogous to increased excitability described previously in the immediate post-SD period (Kawasaki et al., 1988, Jing et al., 1991). As this activity ceased, a secondary phase of synaptic depression developed. Thus, despite the complete recovery of presynaptic fiber volleys within 0.7±0.1 min, postsynaptic potentials were suppressed for a further 6.4±0.4 min (n=6).

These findings imply that, in addition to transient depolarization block of presynaptic action potentials (fiber volleys), another mechanism(s) contributes to the very delayed recovery of postsynaptic potentials after SD.

2. SD characteristics influence secondary suppression

Clinical recordings have shown a correlation between DC shift duration and suppression of electrocorticographic activity (Dreier et al., 2009, Hartings et al., 2011a)). Similarly, the persistence of secondary fEPSP suppression in the current study correlated with the duration of DC shifts (Figure 3A). In addition, the area of tissue recruited into the initial spreading depolarization was positively related to the duration of subsequent fEPSP suppression (Figure 3B). No correlation was seen between the area of tissue involved and the duration of the DC shift (Pearson's R^2=0.02, p=0.65), indicating that these may be independent predictors of fEPSP suppression. These results support the possibility that accumulation of adenosine, a consequence of energetic challenge resulting from SD, could be involved in secondary suppression.

3. Adenosine accumulation

Extracellular adenosine accumulation was measured electrochemically with enzyme-linked probes (combining adenosine deaminase, purine nucleoside phosphorylase and xanthine oxidase; see Experimental Procedures) placed at the slice surface (Figure 4). Large, reproducible increases in electrode signals were observed following SD (Figure 4A). Detectable increases in adenosine signals were first observed 47.9±8.4 s after the peak negative DC potential, when DC shift had recovered to 96.9±0.2% of baseline values (n=6). From comparison with an adenosine standard, endogenous adenosine then reached an estimated peak of 76.6 ± 8.0 μM, and this peak occurred 3.7±0.7 min after the maximum negative DC potential (n=6). Significant elevations persisted for 9.0±1.3 minutes (n=6), encompassing the duration of the secondary phase of synaptic depression described above (Figure 2).

Control studies were consistent with adenosine mediating the bulk of these signals. Thus the reversible adenosine deaminase inhibitor *erythro*-9-(2-hydroxy-3-nonyl)adenine (EHNA, 5 μM) substantially reduced the peak signal after SD and residual electrode responses elicited by SD were indistinguishable from those observed with exogenous adenosine (Fig 4B). These control experiments were performed serially in each slice, alternating the order of EHNA addition/wash out and maintaining 15 min intervals between SD challenges to avoid SD failure (EHNA+SD vs. SD $p<0.05$, EHNA+SD vs. EHNA+adenosine $p>0.05$, paired t-tests with Bonferroni correction for multiple comparisons, n=4).

Signals could not be generated by mechanical manipulations such as deliberate movement of the probe against the slice surface. In addition, EHNA had no effect on IOS changes (area under the curve 274.3±39.2 vs. 271.0±37.5 %×min, EHNA vs. control, p=0.93, paired t-test, n=4), implying that mechanical artifact from tissue swelling associated with SD did not contaminate adenosine electrode studies.

4. Adenosine A1 receptor-mediated secondary suppression

The selective adenosine A1 receptor antagonist DPCPX (500 nM) abolished the secondary phase of synaptic depression (Figure 5). In the presence of DPCPX, SD was induced and verified as described above. There was no effect of DPCPX on the final extent of fEPSP recovery at 15 minutes (104.1±2.5% vs. 102.9±2.6%, DPCPX vs. vehicle, p=0.73, unpaired t-test, n=6). DPCPX also had no effect on fEPSP or presynaptic fiber volley amplitude at baseline (data not shown), and both the duration of fiber volley suppression during SD and the degree of its recovery were unaffected (time suppressed 35.0±2.2 vs. 28.3±3.1 s, DPCPX vs. vehicle, p=0.11, unpaired t-test; recovery to 119.8±8.9 vs. 105.8±7.3% in DPCPX vs. vehicle, p=0.25, unpaired t-test, n=6).

In a separate set of studies, we evaluated whether A1R activation accounted for all the secondary suppression of fEPSPs, after resolution of action potential failure. Fiber volley and fEPSP amplitudes were monitored, and SD was induced in the presence of DPCPX (Figure 6). In this series, fiber volleys recovered fully within 0.9±0.1 min after SD. fEPSP recovery was rapid but not immediate, reaching ≥80% baseline at 3.2±0.7 min ($p<0.05$ vs. fiber volley, paired t-test, n=10). Thus, while fiber volley block and A1R activation explained a large majority of the synaptic suppression following SD, they did not fully account for approximately 2 minutes of depressed fEPSP amplitude.

Figure 7 shows that SD properties were similar between DPCPX and control slices, despite the marked difference in fEPSP recovery. Figure 7A directly illustrates the relationship between the extracellular DC shift and inhibition of fEPSPs. In a control slice, fEPSP suppression outlasted DC shifts by several minutes, whereas in a slice pre-treated with DPCPX, fEPSP recovery began immediately after neutralization of the DC potential. The absence of post-synaptic potentials during the DC shift could be attributed to action potential failure (Figure 1). No differences in IOS were observed (area under the curve 292.7±9.7 vs. 271.5±12.1%×min, vehicle vs. DPCPX, p=0.20, n=6). Figure 7B summarizes lack of effect of DPCPX on the key characteristics of SD (i-iii), and shows that adenosine accumulated to similar levels in the presence of DPCPX (iv).

The results observed in DPCPX were confirmed with another selective A1R antagonist, 8-cyclopentyl-1,3-dimethylxanthine (8-CPT). Like DPCPX, 8-CPT (10 μM) drastically reduced the secondary suppression period (Figure 8A). 8-CPT did not modify SD propagation rates (3.8±0.3 vs. 3.3±0.4 mm/min, vehicle vs. 8-CPT, p=0.34, unpaired t-test, n=6). Post-SD IOS increases were also unchanged by 8-CPT (260.2±23.0 vs. 265.8=0±46.4 %×min, vehicle vs. 8-CPT, p=0.93, unpaired t-test, n=6).

As a positive control, we confirmed that fEPSPs were inhibited (to 11.1±1.8% of baseline) by a selective A1R agonist, CPA (100 nM). A1R activation has been shown to delay SD in metabolically compromised tissue (Canals et al., 2008), but at this concentration CPA did not interfere with SD induction by K^+ microinjection, nor did it slow SD propagation (3.0±0.1 vs. 3.0±0.3 mm/min, CPA vs. control, p=0.93, unpaired t-test, n=6). IOS changes after SD were unaffected by CPA (201.6±8.6 vs. 197.2±36.6 %×min, CPA vs. control, p=0.91, unpaired t-test, n=6). Following SD, CPA-treated slices demonstrated the same sequence of transient fiber volley suppression and initial fEPSP/population spike hyperexcitability as described above. No further suppression of fEPSPs (below that caused by CPA alone) was seen after SD, and minimum fEPSP amplitudes were comparable to vehicle-treated slices (7.6±0.5 vs. 8.5±1.5%, CPA vs. vehicle, p=0.61, unpaired t-test, n=6). Aside from the transient hyperexcitability seen in the immediate post-SD period, no recovery of fEPSPs was seen as long as CPA was maintained in the superfusion medium.

5. Other purinergic receptors

Adenosine released following SD could in principle engage other adenosine receptors in addition to A1Rs. We first assessed A2A receptors, since these have been shown to be activated in CA1 following OGD (Pugliese et al., 2009). Slices were pre-exposed to a selective antagonist, ZM 241385 (500 nM). This drug had no effect on fEPSP recovery (Figure 8B), nor on SD propagation rate (3.3±0.2 vs. 3.0±0.2 mm/min, ZM 241385 vs. vehicle, p=0.36, unpaired t-test, n=6) or IOS signals (221.4±32.9 vs. 229.0±20.1 %×min, ZM 241385 vs. vehicle, p=0.85 unpaired t-test, n=6).

The results described above (Sections 3&4) could also be explained by release of ATP, followed by extracellular degradation to adenosine by NTPDase and ecto-5'-nucleotidase activity (Cunha et al., 1998). We evaluated P2 receptor activation with suramin (50 μM), a nonselective antagonist of P2X and P2Y receptors (Figure 8C). Pre-exposing slices to suramin had no effect on fEPSP recovery, nor on SD propagation rate (3.8±0.2 vs. 3.8±0.3 mm/min, suramin vs. vehicle, p=0.92, unpaired t-test, n=6). IOS signals were not significantly changed by suramin (275.5±21.7 vs. 281.6±15.8 %×min, suramin vs. control, p=0.82 unpaired t-test, n=6).

Together with results in Figures 5&6, these results indicate that activation of A1Rs is the primary contributor to adenosine-mediated secondary depression of fEPSPs after SD.

6. Secondary suppression and refractory period for SD initiation

We considered the possibility that A1-dependent depression of synaptic transmission could influence the susceptibility of tissue to SD generation. Under normal conditions (vehicle), pairs of SDs could be generated reliably at 15 min intervals (6/6 preparations), but failures were seen when the interval between challenges was decreased. Thus pairs of SDs could not be generated at 5 min intervals (0/4 preparations), and at 10 min intervals only 2/8 preparations generated a second SD in vehicle. Pre-exposure of slices to DPCPX did not significantly alter this apparent refractory period. Thus in DPCPX, 0/4 pairs of SDs were observed with 5 min test intervals, despite restoration of synaptic transmission to 86.8±6.9% of baseline. At 10 min inter-stimulus interval, pairs of SDs could be generated in only 4/8 preparations in DPCPX (no significant difference when compared with interleaved vehicle controls, P=0.61, Fisher's exact test). As in vehicle preparations, pairs of SDs were recorded in 6/6 preparations at 15 min intervals in DPCPX. These results suggest that recovery of fEPSPs in DPCPX was not sufficient to overcome the refractoriness of repetitive SDs seen with this KCl microinjection method.

7. Effects on PPR

A1R suppression of evoked transmission can be mediated by both presynaptic and postsynaptic mechanisms (Thompson et al., 1992). We used paired-pulse ratio (PPR) measurements (see Methods) as an indirect assessment of changes in presynaptic release probability after SD. Pairs of presynaptic stimuli were applied at 50ms interpulse intervals. Significant facilitation was observed under control conditions, and prior work has attributed this effect to enhanced Ca^{2+}-dependent probability of vesicle release Quantal analysis supports the involvement of presynaptic, rather than changes in postsynaptic sensitivity (see Zucker and Regehr, 2002). Thus increases in PPR correlate with decreased initial release probability (Thomson, 2000).

As shown in Figure 9, we observed PPR increases after SD, consistent with decreased presynaptic release probability during the period of secondary fEPSP suppression. In vehicle-treated slices, PPR reached a maximum of 2.1±0.1 at 4.8±0.3 min after SD onset (peaks identified individually in 6 preparations). In DPCPX by contrast, PPR increases were

not observed following SD (maximum detected within the same time period 1.5±0.1, $p<0.001$ vs. vehicle, unpaired t-test, n=6). These observations are consistent with a role of presynaptic A1R activation in the sustained suppression of evoked fEPSPs.

Initial PPR decreases were observed in control conditions (without DPCPX), but this period was short and rapidly converted to the longer-lasting PPR increase described above (Fig 8B). A1R-block with DPCPX revealed a longer-lasting PPR decrease after SD (minimum 1.2±0.0 at 3.2±0.4 min, $p<0.01$ vs. baseline, paired t-test), which gradually recovered to baseline values over 5.8±0.7 min (n=6).

Treatment with 8-CPT, as with DPCPX, abolished PPR increases after SD (maximum 1.5±0.1 vs. 2.0±0.1, 8-CPT vs. vehicle, $p<0.01$, unpaired t-test, n=6). Overshoots of PPR were observed for slices treated with ZM 241385, and changes were indistinguishable from vehicle (maximum 1.8±0.1 vs. 2.0±0.2, ZM vs. vehicle, p=0.74, unpaired t-test). PPR was also elevated following SD in the presence of suramin (maximum 1.9±0.0 vs. 2.0±0.1, suramin vs. control, p=0.20, unpaired t-test, n=6). Slices treated with CPA had elevated PPR at baseline (2.0±0.1 vs. 1.5±0.0, CPA vs. control, $p<0.01$, unpaired t-test, n=6) and after SD, PPR decreased in CPA and increased in control such that the values were indistinguishable between treatments. This series of studies suggests that A1R activation reduces the presynaptic release probability during secondary suppression, and that another process normally masked by adenosine increases the probability of release early after SD.

DISCUSSION

General

This study provides evidence that depression of synaptic transmission following spreading depolarization in brain slices is not only due to depolarization block. Only an initial brief period of suppression associated with the DC shift was marked by failure of presynaptic action potentials. A longer-lasting synaptic depression was accompanied by adenosine accumulation and appeared to be due mainly to activation of A1Rs. PPR changes were consistent with a presynaptic site of action. The correlation between persistence of synaptic suppression and the duration of DC shifts and the volume of tissue involved is consistent with a model in which metabolic depletion following SD is responsible for extracellular adenosine accumulation.

Depolarization block

TTX-sensitive fiber volleys were abolished during SD, approximately matching the duration of the DC shift. These data support the model that the initial phase of synaptic depression might be attributable to collapse of ionic gradients and/or intrinsic inactivation of voltage-gated sodium channels during SD (see discussion in Kager et al., 2000). In the present study, such depolarization block accounted for an absolute refractory period of approximately 30–40 seconds, during which time neither pre- nor post-synaptic potentials could be evoked (Figures 1, 2, & 7). The fact that fiber volleys and fEPSPs recovered rapidly after the DC shift (in the presence of A1R antagonists) implies that the major ionic gradients establishing resting membrane potential, neuronal excitability, and vesicular release were largely intact soon after SD.

The recovery of fiber volleys seen here is earlier than previously described in studies in which SD was induced by either simulated ischemia or continuous superfusion with elevated K^+ solutions (Kawasaki et al., 1988, Frenguelli et al., 2007). Prolonged neuronal depolarization related to the global stimuli in prior studies (in addition to the propagating SD event itself) could account for the more delayed recoveries of fiber volleys. In the current study, SD was generated by focal microinjections of KCl at a relatively long distance from

the recording site (~0.5 mm), and thus the stimulus did not interfere directly with the duration of the SD depolarization at the recording site.

Synaptic transmission often transiently recovered immediately following recovery of the DC shift, with events resembling population spikes. These events were observed between depolarization block and secondary suppression of transmission. EPSP-spike potentiation has previously been described following SD (or conditions expected to generate SD) in hippocampal slices (Kawasaki et al., 1988, Jing et al., 1991, Park et al., 2003) and *in vivo* (Herreras and Somjen, 1993). These events could also relate to other forms of hyperexcitability previously reported to follow SD, including seizure-like activity (Van Harreveld and Stamm, 1953, Gorji and Speckmann, 2004, Dreier et al., 2012). In the current study, breakthrough of synaptic activity between depolarization block and secondary suppression was independent of adenosine accumulation, as it was unaffected by A1R antagonists DPCPX and 8-CPT (see Figures 5&8) and also persisted in the presence of the A1R agonist CPA.

Adenosine release and A1 receptor-mediated suppression

Significant adenosine accumulation was associated with SD, consistent with previous microdialysis recordings of SD from hippocampus *in vivo* (Kaku et al., 1994) and hippocampal slices following AD (Frenguelli et al., 2007). In the current study adenosine appeared to activate A1Rs, which accounted for a large majority of the secondary fEPSP suppression after SD. A1R block did not reduce adenosine accumulation, and other purinergic receptors (namely A2ARs and P2Rs) were not involved in suppression or recovery of fEPSPs. In the presence of A1R antagonists, recovery of fEPSP amplitude was quite rapid, but not immediate. A third mechanism is likely involved, to account for the slight remaining delay of fEPSP recovery after depolarization block in the presence of A1R antagonists. A number of mechanisms could potentially contribute, including decreased postsynaptic membrane resistance (shunting), or depletion of presynaptic vesicle number or neurotransmitter content.

This work builds on a previous report that transient A1R-mediated suppression of fEPSPs at Schaffer collateral-CA1 synapses occurred after prolonged (up to 7 min) superfusion with elevated K^+ solutions (Park et al., 2003), a treatment that likely induced SD (see similar methods in Kawasaki et al., 1988, Zhou et al., 2010). However, such prolonged K^+ exposures and neuronal activation could elicit adenosine release without SD (Dunwiddie and Masino, 2001). Inhibition of glial oxidative metabolism quickly gives rise to adenosine accumulation and A1R-dependent EPSP suppression, which occludes any effect of adenosine that might be released by SD (Canals et al., 2008). The findings presented here demonstrate that adenosine accumulates to functionally significant levels even in the presence of 95% oxygen and 10 mM glucose, at basal K^+ concentrations (3 mM), and can therefore be attributed to consequences of SD itself.

Inhibition of Ca^{2+} influx and glutamate release by presynaptic A1Rs is well established (Dunwiddie and Masino, 2001), and PPR results here are fully consistent with this being a major mechanism after SD. Thus significant increases in PPR (interpreted as decreases in presynaptic release probability, see Results) occurred during the time of secondary suppression, and were abolished by A1R antagonists. In addition, A1R activation has been reported to increase postsynaptic K^+ conductance and result in membrane hyperpolarization in hippocampal slice cultures (Thompson et al., 1992). A1R-mediated postsynaptic changes could also contribute to some extent to secondary suppression, together with the strong presynaptic actions.

A period of *increased* presynaptic release probability (PPR decrease) was also noted after SD, (Figure 9) and this period was enhanced by A1R block. The underlying mechanism(s) of increased initial release probability could include elevated residual Ca^{2+} in presynaptic terminals and/or sensitization of release machinery. The present study raises the possibility that adenosine accumulation may counteract presynaptic hyperexcitability to some extent in the post-SD period.

Source(s) of adenosine

Adenosine and other metabolites may accumulate in the extracellular space as a consequence of the demands of ion pumping (and other cellular processes) throughout the affected tissue. Indeed, metabolic demand after SD appears to cause tissue hypoxia *in vitro* (Galeffi et al., 2011) and to exceed the supportive capacity of the vascular supply, resulting in hypoxia, hypoglycemia, and hyperlactatemia *in vivo* (Takano et al., 2007, Lauritzen et al., 2011, Yuzawa et al., 2012). However, non-metabolic ATP release from astrocytes or neurons likely also plays a role in regulating synaptic transmission in this phase (Frenguelli et al., 2007, Schock et al., 2007). We report a correlation between A1R-mediated suppression and the duration and spatial extent of SD, which would be consistent with a metabolic source of adenosine. The form, cellular sources, and routes of adenosine release may be important to elucidate in future studies, to help to guide strategies to assess and prevent metabolic depletion associated with SD under some conditions.

Relationship to Cortical Spreading Depression (CSD)

The present *in vitro* study provides evidence that depolarization block and A1R-mediated neuronal inhibition are candidate mechanisms that may contribute to spreading depression of cortical activity following SD in vivo. However, the relative contributions of each remain to be investigated in cortical spreading depression (CSD). A variety of approaches might be needed to assess depolarization block and A1R-mediated suppression *in vivo*. Topical delivery of pharmacological agents might accelerate cortical responsiveness to electrically-evoked local field potentials, yet without accelerating recovery of the electrocorticogram, as propagation of SD into subcortical structures (Eikermann-Haerter et al., 2009) can disrupt afferent cortical inputs (Bures et al., 1974). Adenosine accumulation *in vivo* may also affect blood flow through activation of vascular A2A receptors (Ngai et al., 2001), possibly confounding interpretation of electrophysiological results.

Relationship to metabolic status and injury

The Cooperative Studies on Brain Injury Depolarizations (CoSBID) group has accumulated substantial clinical and experimental data indicate that in the injured brain, delayed or incomplete recovery of DC potential is associated with progression of injury and poor clinical outcomes (Oliveira-Ferreira et al., 2010, Hartings et al., 2011b)). A correlation between DC shift duration and suppression of the spontaneous electrocorticogram has previously been reported in clinical case series (Dreier et al., 2009, Hartings et al., 2011b)). The present study employed non-injurious SD stimuli in healthy brain slices, to better describe the relationship of the DC shift to synaptic depression. Although the DC shifts observed here were quite short (<1 min) and non-injurious, we also observed a relationship between DC shift duration and secondary suppression of evoked potentials, which we identified as a period of A1R activation.

By reducing neuronal excitability, adenosine associated with SD may reduce extracellular accumulation of glutamate and K^+ to delay SD under some conditions. Previous work implies that adenosine accumulation can delay the spontaneous generation of SD in fluoroacetate (Canals et al., 2008) and reduce the frequency of SD generated by continuous application of KCl *in vivo* (Kaku et al., 1994). In both these prior studies, the average

frequency of spontaneously-generated SDs was low, and the inter-SD interval was much longer (~18–30min) than the adenosine accumulation described in the present study. Even with A1R block, average inter-SD intervals were maintained above 10 min (Kaku et al., 1994, Canals et al., 2008). Consistent with these observations, we did not detect an A1R-dependent component of refractoriness to repetitive SD, when generated by pairs of KCl stimuli at 5–10 minute intervals. These observations suggest that recovery of fEPSPs in DPCPX was not sufficient to overcome the refractoriness of repetitive SDs seen with this KCl microinjection method, and more substantial adenosine accumulations generated in the context of injury or sustained exposure to metabolic stressors may be required to increase inter-SD intervals. Endogenous and/or exogenous adenosine may have other beneficial consequences, including improving neurovascular coupling and reducing the duration of DC shifts (Dreier et al., 2004). It remains to be determined whether adenosine accumulation and synaptic suppression may modulate neuronal injury associated with prolonged DC shifts in clinical settings.

Conclusion

This study provides a mechanism for one significant consequence of SD, spreading depression of evoked synaptic activity. After a short period of depolarization block associated with the DC shift, adenosine accumulates in the extracellular space, and subsequent A1R activation appears to be the predominant mediator of sustained synaptic inhibition. A1R activation may link metabolic depletion with functional recovery, and may complement measures of DC shifts in predicting tissue viability following SD.

Acknowledgments

Supported by NIH grants NS051288 (C.W.S.) and T32HL007736 & F31NS078805 (B.E.L.). The authors thank Drs L.D. Prtridge and C.F. Valenzuela for helpful feedback on drafts of this manuscript.

ABBREVIATIONS

8-CPT	8-cyclopentyl-1,3-dimethylxanthine
A1R	adenosine A1 receptor
aCSF	artificial cerebrospinal fluid
AD	anoxic depolarization
ATP	adenosine 5’ triphosphate
CA1	Cornu Ammonis area 1
CPA	6-cyclopentyl adenosine
CSD	cortical spreading depression
DC	direct current
DMSO	dimethyl sulfoxide
DNQX	6,7-dinitroquinoxaline-2,3-dione
DPCPX	8-cyclopentyl-1,3-dipropylxanthine
EHNA	*erythro*-9-(2-hydroxy-3-nonyl)adenine hydrochloride
fEPSP	field excitatory postsynaptic potential
IOS	intrinsic optical signal
KCl	potassium chloride

OGD	oxygen-glucose deprivation
PPR	paired-pulse ratio
SD	spreading depolarization
TTX	tetrodotoxin
ZM 241385	4-(-2-[7-amino-2-(2-furyl)(1,2,4)triazolo(2,3-a)(1,3,5triazin-5-yl-amino]ethyl)phenol

REFERENCES

Andrew RD, Jarvis CR, Obeidat AS. Potential sources of intrinsic optical signals imaged in live brain slices. Methods. 1999; 18:185–196. 179. [PubMed: 10356350]

Back T, Ginsberg MD, Dietrich WD, Watson BD. Induction of spreading depression in the ischemic hemisphere following experimental middle cerebral artery occlusion: effect on infarct morphology. J Cereb Blood Flow Metab. 1996; 16:202–213. [PubMed: 8594051]

Bures, J.; Buresova, O.; Krivanek, J. The Mechanism and Applications of Leao's Spreading Depression of Electroencephalographic Activity. Prague, Czechoslovakia: Academia; 1974.

Canals S, Larrosa B, Pintor J, Mena MA, Herreras O. Metabolic challenge to glia activates an adenosine-mediated safety mechanism that promotes neuronal survival by delaying the onset of spreading depression waves. J Cereb Blood Flow Metab. 2008; 28:1835–1844. [PubMed: 18612316]

Dale N, Frenguelli BG. Measurement of purine release with microelectrode biosensors. Purinergic Signal. 2012; 8:27–40. [PubMed: 22095158]

Dreier JP. The role of spreading depression, spreading depolarization and spreading ischemia in neurological disease. Nat Med. 2011; 17:439–447. [PubMed: 21475241]

Dreier JP, Major S, Manning A, Woitzik J, Drenckhahn C, Steinbrink J, Tolias C, Oliveira-Ferreira AI, Fabricius M, Hartings JA, Vajkoczy P, Lauritzen M, Dirnagl U, Bohner G, Strong AJ. Cortical spreading ischaemia is a novel process involved in ischaemic damage in patients with aneurysmal subarachnoid haemorrhage. Brain. 2009; 132:1866–1881. [PubMed: 19420089]

Dreier JP, Major S, Pannek HW, Woitzik J, Scheel M, Wiesenthal D, Martus P, Winkler MK, Hartings JA, Fabricius M, Speckmann EJ, Gorji A. Spreading convulsions, spreading depolarization and epileptogenesis in human cerebral cortex. Brain. 2012; 135:259–275. [PubMed: 22120143]

Dreier JP, Tille K, Dirnagl U. Partial antagonistic effect of adenosine on inverse coupling between spreading neuronal activation and cerebral blood flow in rats. Neurocrit Care. 2004; 1:85–94. [PubMed: 16174901]

Dunwiddie TV, Masino SA. The role and regulation of adenosine in the central nervous system. Annu Rev Neurosci. 2001; 24:31–55. [PubMed: 11283304]

Eikermann-Haerter K, Dileköz E, Kudo C, Savitz SI, Waeber C, Baum MJ, Ferrari MD, van den Maagdenberg AM, Moskowitz MA, Ayata C. Genetic and hormonal factors modulate spreading depression and transient hemiparesis in mouse models of familial hemiplegic migraine type 1. J Clin Invest. 2009; 119:99–109. [PubMed: 19104150]

Fowler JC. Adenosine antagonists delay hypoxia-induced depression of neuronal activity in hippocampal brain slice. Brain Res. 1989; 490:378–384. [PubMed: 2765871]

Frenguelli BG, Wigmore G, Llaudet E, Dale N. Temporal and mechanistic dissociation of ATP and adenosine release during ischaemia in the mammalian hippocampus. J Neurochem. 2007; 101:1400–1413. [PubMed: 17459147]

Galeffi F, Somjen GG, Foster KA, Turner DA. Simultaneous monitoring of tissue PO2 and NADH fluorescence during synaptic stimulation and spreading depression reveals a transient dissociation between oxygen utilization and mitochondrial redox state in rat hippocampal slices. J Cereb Blood Flow Metab. 2011; 31:626–639. [PubMed: 20736960]

Gorji A, Speckmann EJ. Spreading depression enhances the spontaneous epileptiform activity in human neocortical tissues. Eur J Neurosci. 2004; 19:3371–3374. [PubMed: 15217393]

Hartings JA, Bullock MR, Okonkwo DO, Murray LS, Murray GD, Fabricius M, Maas AI, Woitzik J, Sakowitz O, Mathern B, Roozenbeek B, Lingsma H, Dreier JP, Puccio AM, Shutter LA, Pahl C, Strong AJ. Spreading depolarisations and outcome after traumatic brain injury: a prospective observational study. Lancet neurology. 2011a; 10:1058–1064. [PubMed: 22056157]

Hartings JA, Rolli ML, Lu XC, Tortella FC. Delayed secondary phase of peri-infarct depolarizations after focal cerebral ischemia: relation to infarct growth and neuroprotection. J Neurosci. 2003; 23:11602–11610. [PubMed: 14684862]

Hartings JA, Watanabe T, Bullock MR, Okonkwo DO, Fabricius M, Woitzik J, Dreier JP, Puccio A, Shutter LA, Pahl C, Strong AJ. Spreading depolarizations have prolonged direct current shifts and are associated with poor outcome in brain trauma. Brain. 2011b; 134:1529–1540. [PubMed: 21478187]

Herreras O, Somjen GG. Effects of prolonged elevation of potassium on hippocampus of anesthetized rats. Brain Res. 1993; 617:194–204. [PubMed: 8402147]

Jing J, Aitken PG, Somjen GG. Lasting neuron depression induced by high potassium and its prevention by low calcium and NMDA receptor blockade. Brain Res. 1991; 557:177–183. [PubMed: 1660751]

Kager H, Wadman WJ, Somjen GG. Simulated seizures and spreading depression in a neuron model incorporating interstitial space and ion concentrations. J Neurophysiol. 2000; 84:495–512. [PubMed: 10899222]

Kaku T, Hada J, Hayashi Y. Endogenous adenosine exerts inhibitory effects upon the development of spreading depression and glutamate release induced by microdialysis with high K+ in rat hippocampus. Brain Res. 1994; 658:39–48. [PubMed: 7834353]

Kawasaki K, Czeh G, Somjen GG. Prolonged exposure to high potassium concentration results in irreversible loss of synaptic transmission in hippocampal tissue slices. Brain Res. 1988; 457:322–329. [PubMed: 2851366]

Lauritzen M, Dreier JP, Fabricius M, Hartings JA, Graf R, Strong AJ. Clinical relevance of cortical spreading depression in neurological disorders: migraine, malignant stroke, subarachnoid and intracranial hemorrhage, and traumatic brain injury. J Cereb Blood Flow Metab. 2011; 31:17–35. [PubMed: 21045864]

Leao AAP. Spreading depression of activity in the cerebral cortex. Journal of Neurophysiology. 1944; 7:359–390.

Lindquist, BE.; Shuttleworth, CW. Program No. 780.02 2011 Neuroscience Meeting Planner. Washington, DC: Society for Neuroscience; 2011. Adenosine activation of A1 receptors depresses synaptic activity after spreading depolarization.

Mies G, Paschen W. Regional changes of blood flow, glucose, and ATP content determined on brain sections during a single passage of spreading depression in rat brain cortex. Exp Neurol. 1984; 84:249–258. [PubMed: 6714339]

Mitchell JB, Lupica CR, Dunwiddie TV. Activity-dependent release of endogenous adenosine modulates synaptic responses in the rat hippocampus. J Neurosci. 1993; 13:3439–3447. [PubMed: 8393482]

Muller M, Somjen GG. Na(+) dependence and the role of glutamate receptors and Na(+) channels in ion fluxes during hypoxia of rat hippocampal slices. J Neurophysiol. 2000; 84:1869–1880. [PubMed: 11024079]

Ngai AC, Coyne EF, Meno JR, West GA, Winn HR. Receptor subtypes mediating adenosineinduced dilation of cerebral arterioles. Am J Physiol Heart Circ Physiol. 2001; 280:H2329–H2335. [PubMed: 11299238]

Oliveira-Ferreira AI, Milakara D, Alam M, Jorks D, Major S, Hartings JA, Lückl J, Martus P, Graf R, Dohmen C, Bohner G, Woitzik J, Dreier JP, group Cs. Experimental and preliminary clinical evidence of an ischemic zone with prolonged negative DC shifts surrounded by a normally perfused tissue belt with persistent electrocorticographic depression. J Cereb Blood Flow Metab. 2010; 30:1504–1519. [PubMed: 20332797]

Park YK, Shim ES, Oh JI, Kim JH, Chung YG. Adenosine-mediated synaptic depression and EPSP/spike dissociation following high potassium-induced depolarization in rat hippocampal slices. Brain Res. 2003; 975:237–243. [PubMed: 12763613]

Pugliese AM, Traini C, Cipriani S, Gianfriddo M, Mello T, Giovannini MG, Galli A, Pedata F. The adenosine A2A receptor antagonist ZM241385 enhances neuronal survival after oxygen-glucose deprivation in rat CA1 hippocampal slices. Br J Pharmacol. 2009; 157:818–830. [PubMed: 19422385]

Schock SC, Munyao N, Yakubchyk Y, Sabourin LA, Hakim AM, Ventureyra EC, Thompson CS. Cortical spreading depression releases ATP into the extracellular space and purinergic receptor activation contributes to the induction of ischemic tolerance. Brain Res. 2007; 1168:129–138. [PubMed: 17706620]

Selman WR, Lust WD, Pundik S, Zhou Y, Ratcheson RA. Compromised metabolic recovery following spontaneous spreading depression in the penumbra. Brain Res. 2004; 999:167–174. [PubMed: 14759495]

Shinohara M, Dollinger B, Brown G, Rapoport S, Sokoloff L. Cerebral glucose utilization: local changes during and after recovery from spreading cortical depression. Science. 1979; 203:188–190. [PubMed: 758688]

Shuttleworth CW, Brennan AM, Connor JA. NAD(P)H fluorescence imaging of postsynaptic neuronal activation in murine hippocampal slices. J Neurosci. 2003; 23:3196–3208. [PubMed: 12716927]

Somjen GG. Mechanisms of spreading depression and hypoxic spreading depression-like depolarization. Physiological reviews. 2001; 81:1065–1096. [PubMed: 11427692]

Somjen GG, Aitken PG, Balestrino M, Herreras O, Kawasaki K. Spreading depression-like depolarization and selective vulnerability of neurons. A brief review. Stroke. 1990; 21:III179–III183. [PubMed: 2237979]

Somjen GG, Giacchino JL. Potassium and calcium concentrations in interstitial fluid of hippocampal formation during paroxysmal responses. J Neurophysiol. 1985; 53:1098–1108. [PubMed: 3998794]

Takano T, Tian GF, Peng W, Lou N, Lovatt D, Hansen AJ, Kasischke KA, Nedergaard M. Cortical spreading depression causes and coincides with tissue hypoxia. Nature neuroscience. 2007; 10:754–762.

Thompson SM, Haas HL, Gähwiler BH. Comparison of the actions of adenosine at pre- and postsynaptic receptors in the rat hippocampus in vitro. J Physiol. 1992; 451:347–363. [PubMed: 1403815]

Thomson AM. Facilitation, augmentation and potentiation at central synapses. Trends Neurosci. 2000; 23:305–312. [PubMed: 10856940]

Van Harreveld A, Stamm JS. Spreading cortical convulsions and depressions. J Neurophysiol. 1953; 16:352–366. [PubMed: 13070047]

Wernsmann B, Pape HC, Speckmann EJ, Gorji A. Effect of cortical spreading depression on synaptic transmission of rat hippocampal tissues. Eur J Neurosci. 2006; 23:1103–1110. [PubMed: 16553774]

Wu J, Fisher RS. Hyperthermic spreading depressions in the immature rat hippocampal slice. J Neurophysiol. 2000; 84:1355–1360. [PubMed: 10980008]

Yuzawa I, Sakadzic S, Srinivasan VJ, Shin HK, Eikermann-Haerter K, Boas DA, Ayata C. Cortical spreading depression impairs oxygen delivery and metabolism in mice. J Cereb Blood Flow Metab. 2012; 32:376–386. [PubMed: 22008729]

Zhou N, Gordon GR, Feighan D, MacVicar BA. Transient swelling, acidification, and mitochondrial depolarization occurs in neurons but not astrocytes during spreading depression. Cereb Cortex. 2010; 20:2614–2624. [PubMed: 20176688]

Zucker RS, Regehr WG. Short-term synaptic plasticity. Annu Rev Physiol. 2002; 64:355–405. [PubMed: 11826273]

HIGHLIGHTS

- We examined suppression of synaptic potentials following spreading depolarization.
- Initial inhibition was explained by a short period of action potential failure.
- Presynaptic A1 receptor activation was responsible for the majority of suppression.
- Accumulation of adenosine may link metabolic demand of SD with synaptic depression.

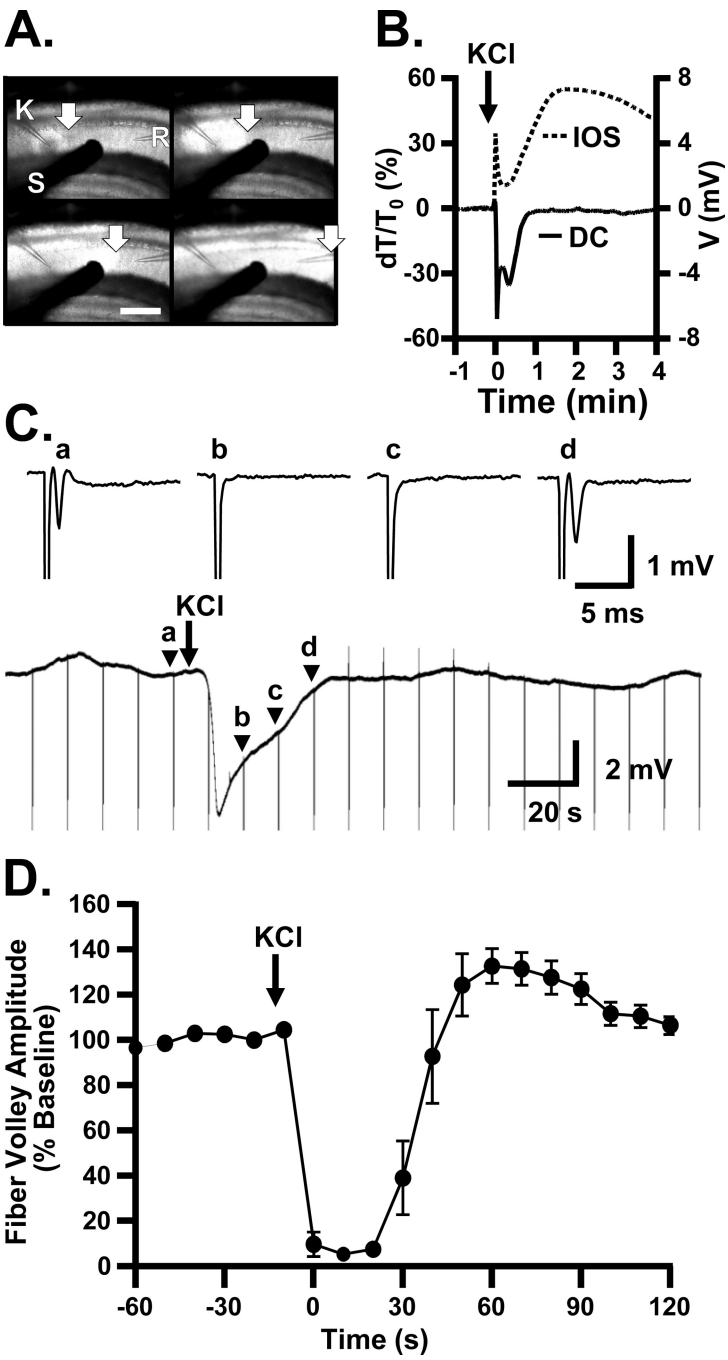

Figure 1. Induction of SD leads to transient loss of fiber volleys, lasting throughout the negative phase of the DC shift

A: Recordings from a representative slice demonstrating electrode positioning and light transmission changes during SD propagation. SD was induced in CA1 by localized KCl microinjection from a glass micropipette (K), achieved by a short pressure pulse (60 ms). Electrical responses were recorded with an aCSF-filled glass microelectrode **(R)**. Test pulses were delivered with a concentric bipolar stimulating electrode **(S)**, to assess evoked potentials. A sharp increase in light transmission (intrinsic optical signal, IOS) marks the propagation of the advancing SD wave (arrows). Scale bar = 320 μm, 4 s interval between frames. **B:** Example of simultaneous arrival of IOS wave front (dashed line) and negative

DC deflection (solid line) characterizing SD. Throughout this study, every SD was confirmed with one or both of these measures. **C:** Example of suppression of fiber volleys during SD. A continuous recording is shown, to illustrate both the slow DC shift occurring after KCl microinjection, and timing of fiber volley stimulation (0.1 Hz test pulses, downward deflections are stimulus artifacts) in the presence of DNQX (10 μM) to isolate fiber volleys. Above: traces from the time points indicated in continuous recording: (**a**) Baseline response, immediately before induction of SD; (**b** and **c**) during the DC shift; (**d**) as extracellular DC potential recovers to baseline. **D**: Mean data from 6 experiments, demonstrating the transient loss of fiber volley after SD ($p<0.001$, ANOVA with Bonferroni post-hoc test, baseline vs. 0, 10, 20, and 30s after initial depolarization, n=6). In these slices, DNQX was not included, and fiber volleys were identified from their timing and waveform.

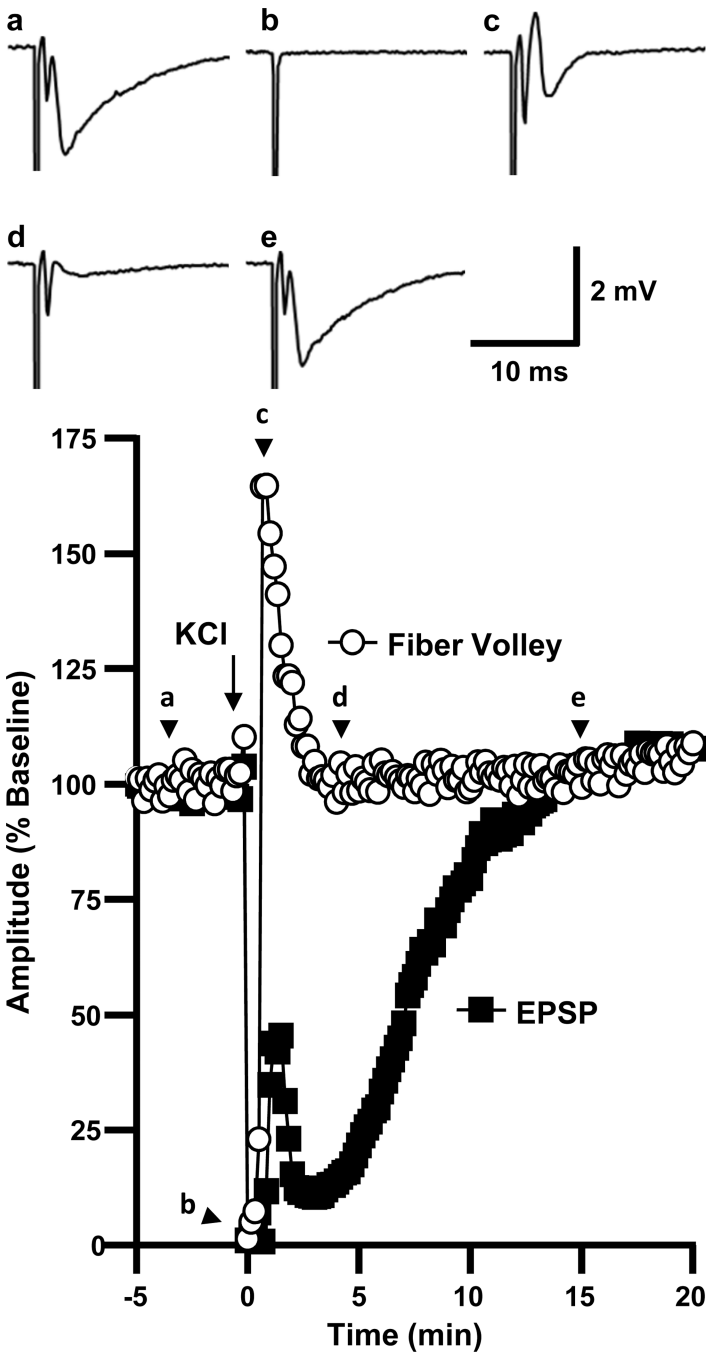

Figure 2. Fiber volley recovers several minutes before postsynaptic potentials

The plot shows the time courses of evoked responses in a representative slice. Presynaptic fiber volley recovery was seen early after SD, while fEPSP recovery was delayed by several minutes. The traces show evoked responses from the same slice, (**a**) at baseline, (**b**) during SD, (**c**) 70s after SD (population spike/transient hyperexcitability), (**d**) 3 minutes after SD (secondary suppression), and (**e**) 15 minutes after SD.

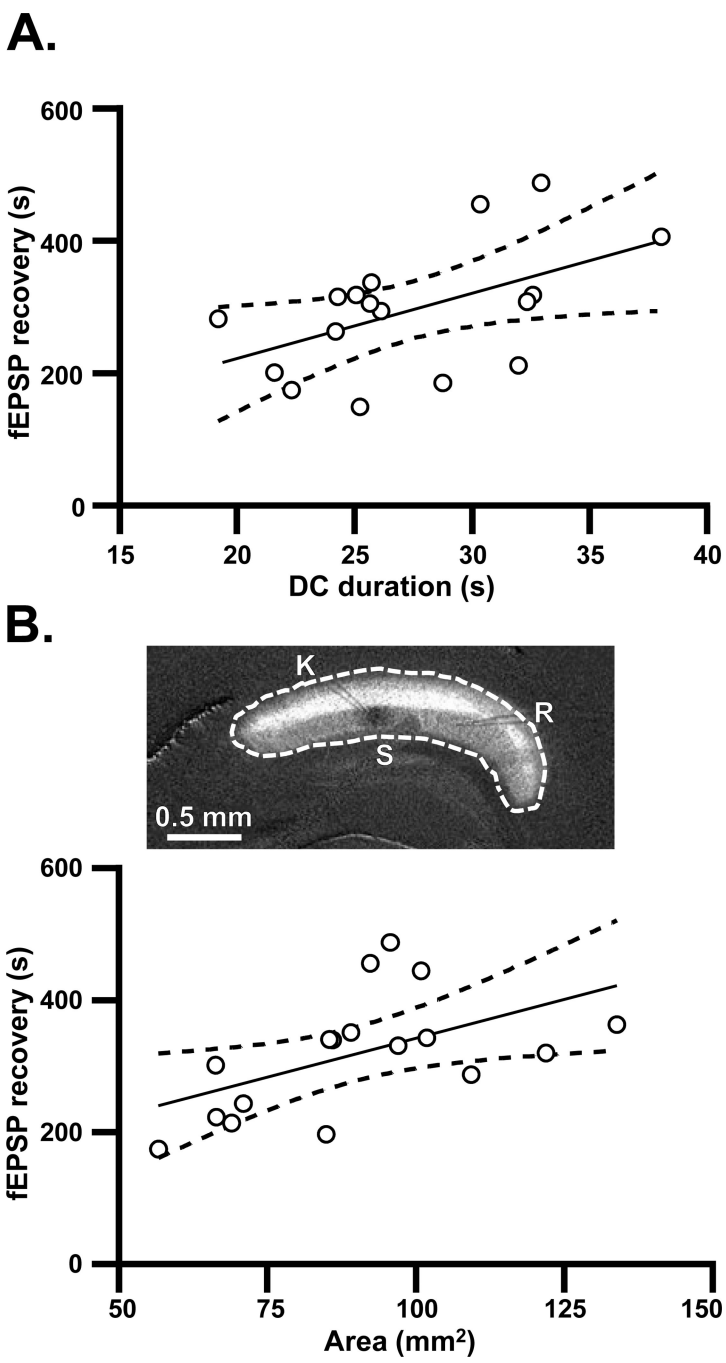

Figure 3. Relationship of DC shifts and spatial extent of SD to the secondary phase of synaptic suppression

A: Relationship between the duration of the DC shift and duration of secondary suppression of fEPSP amplitude. No antagonists were present in these studies, and DC durations and fEPSP recovery times were calculated as described in Experimental Procedures. Solid line: linear regression (Pearson's R^2=0.26, $p<0.05$, n=15). Dashed lines: 95% confidence intervals. **B:** Data from the same preparations as plotted in A, showing that the duration of fEPSP recovery was also predicted by the area of tissue recruited into SD (Pearson's R^2=0.29, $p<0.05$, n=15). The image illustrates how the spatial extent of SD was determined,

from enhanced images of IOS ($\Delta T/T_0$). The perimeter was traced (dotted white line) and the enclosed area was calculated in NIH ImageJ (see Experimental Procedures).

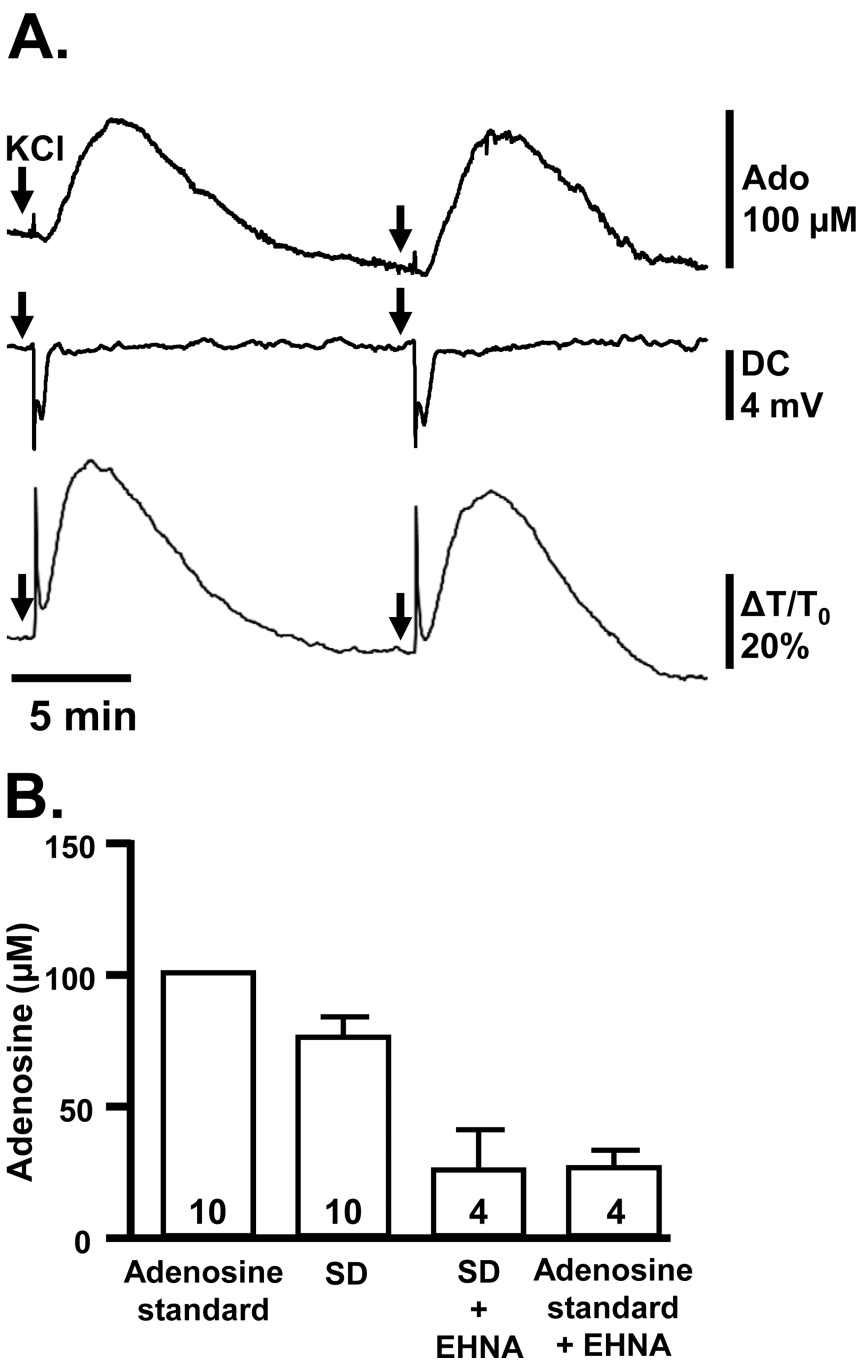

Figure 4. Reproducible large adenosine signals are detected after SD

A: Simultaneous recordings of adenosine probe signals, DC potential, and IOS demonstrating the time course of adenosine detection at the slice surface following the arrival of SD. Two SDs are shown, generated by localized KCl microinjections (arrows). **B:** Summary data showing the maximum estimated adenosine concentration detected after SD, calculated by reference to a 100 µM adenosine standard solution. Signals after SD and responses to the adenosine standard were similarly reduced (by 68.8±5.6% and 73.9±6.5%, respectively) by inclusion of EHNA (5 µM), an inhibitor of adenosine deaminase. Numbers in bars indicate numbers of slices (see Results).

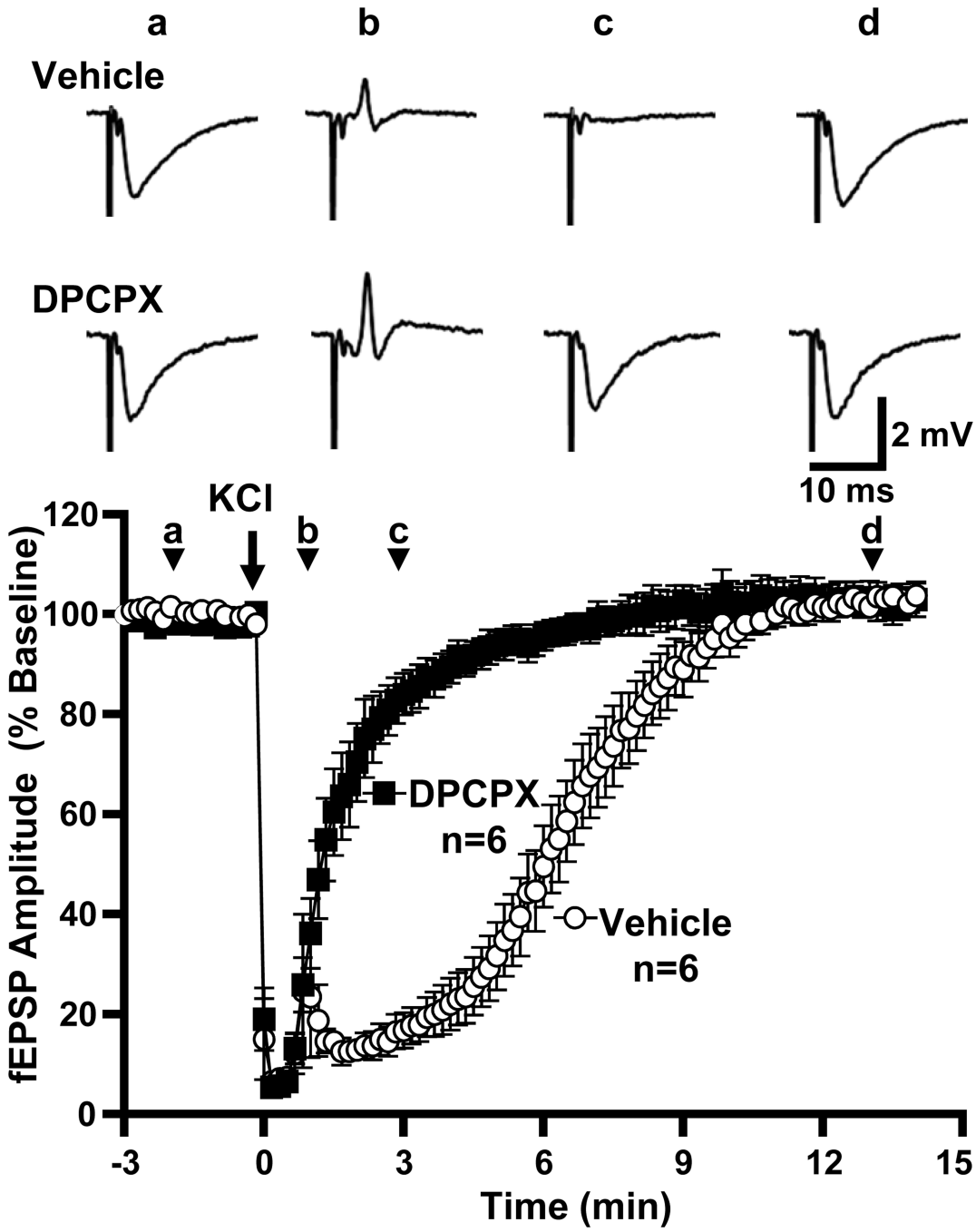

Figure 5. An A1R antagonist greatly accelerates recovery of postsynaptic potentials after SD

The plot shows the time courses of evoked responses in populations of slices, pre-exposed to either DPCPX (500 nM) or vehicle. Vehicle-treated slices displayed the characteristic delayed recovery of postsynaptic potentials observed in Figure 2, while in DPCPX-treated slices postsynaptic potentials recovered almost immediately after SD (t_{50} 1.6±0.2 vs. 6.3±0.5 min, DPCPX vs. interleaved vehicle controls, $p<0.0001$, unpaired t-test, n=6). Shown above are representative traces from one vehicle-treated and one DPCPX-treated slice at (**a**) baseline, (**b**) 1 minute after SD, (**c**) 3 minutes after SD and (**d**) after recovery.

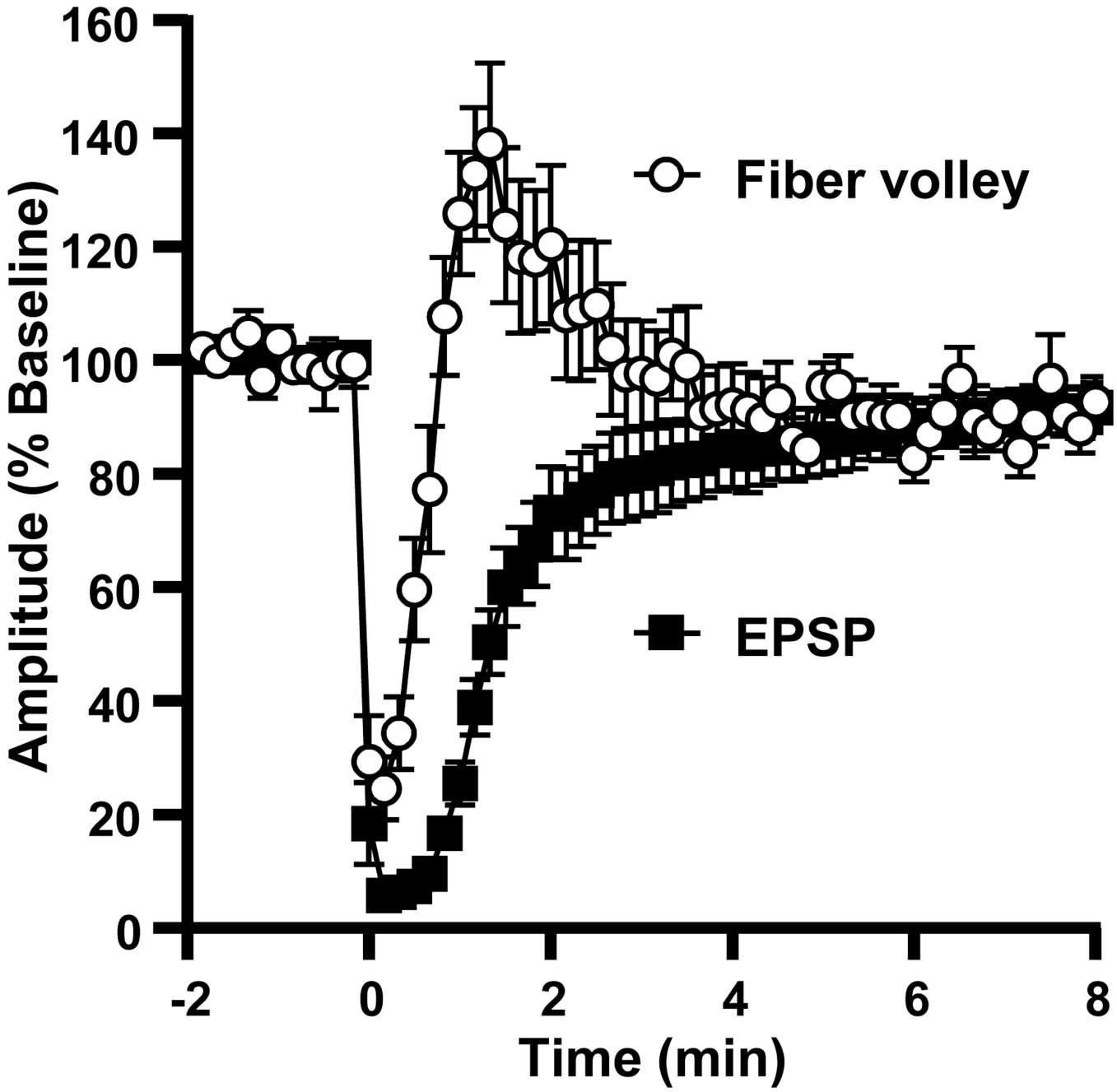

Figure 6. Recovery of fiber volley precedes recovery of fEPSPs with A1R block
Mean data from 10 preparations pre-exposed to DPCPX (500 nM), showing the fiber volley and fEPSP amplitudes normalized to pre-SD amplitudes in each preparation.

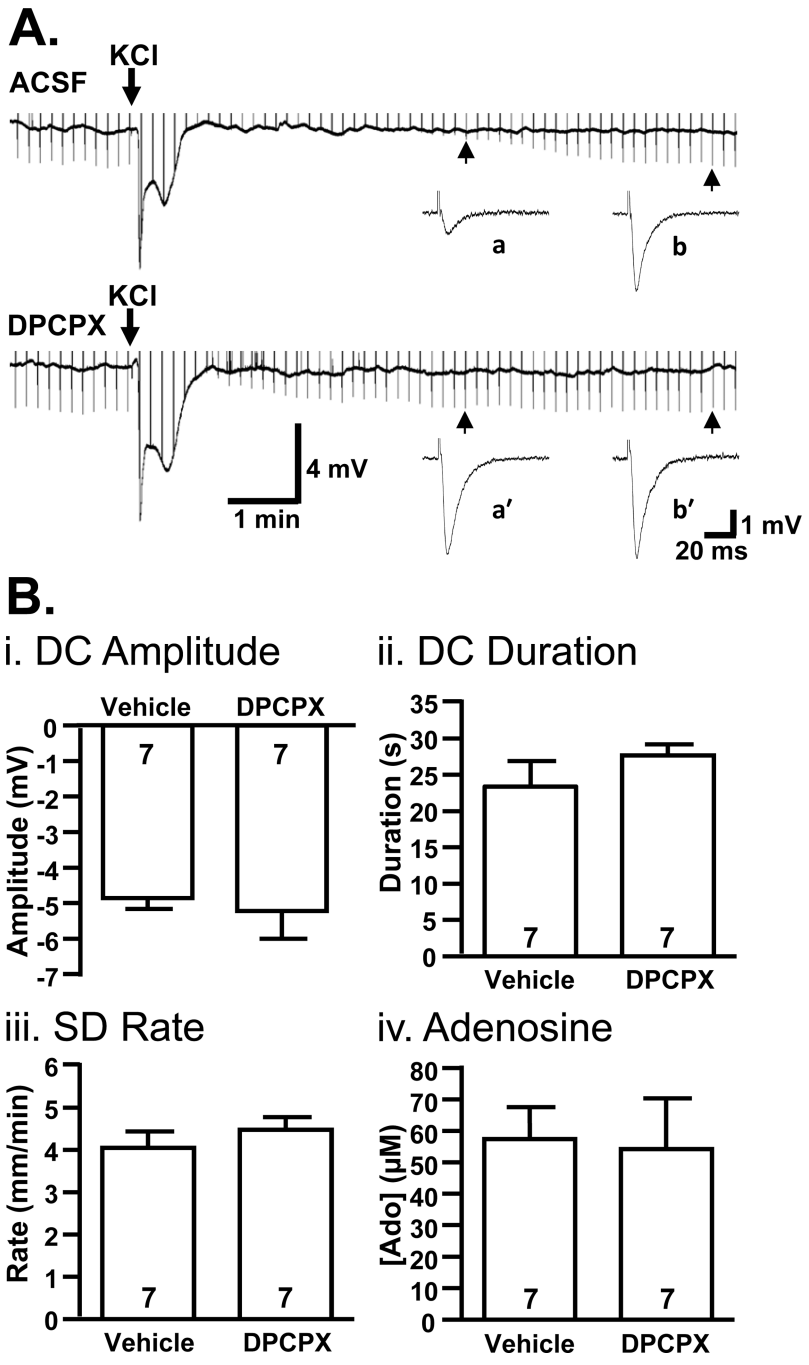

Figure 7. Properties of spreading depolarization are unchanged by A1R antagonist DPCPX

A: Representative continuous recordings show that fEPSPs do not begin to recover until after recovery of the DC shift, even when A1Rs are blocked with DPCPX (500 nM). In these recordings, fEPSPs evoked at 0.1 Hz are illustrated as downward-going deflections in the continuous trace (upward-going stimulus artifacts are truncated). Sample evoked field potentials are also shown at an expanded time scale for both aCSF (**a,b**) and DPCPX-treated slices (**a',b'**). **B:** Each plot compares a characteristic of SD in interleaved studies of slices pre-exposed to DPCPX (500 nM) or vehicle. **i:** DPCPX exposure had no significant effect on the peak negative amplitude of DC shifts (p=0.68), **ii:** the duration of DC shifts

(measured from peak to 80% recovery, p=0.29), or **iii:** SD propagation rate (p=0.40). **iv:** Estimated adenosine (Ado) accumulation was also unaffected by DPCPX treatment (p=0.87).

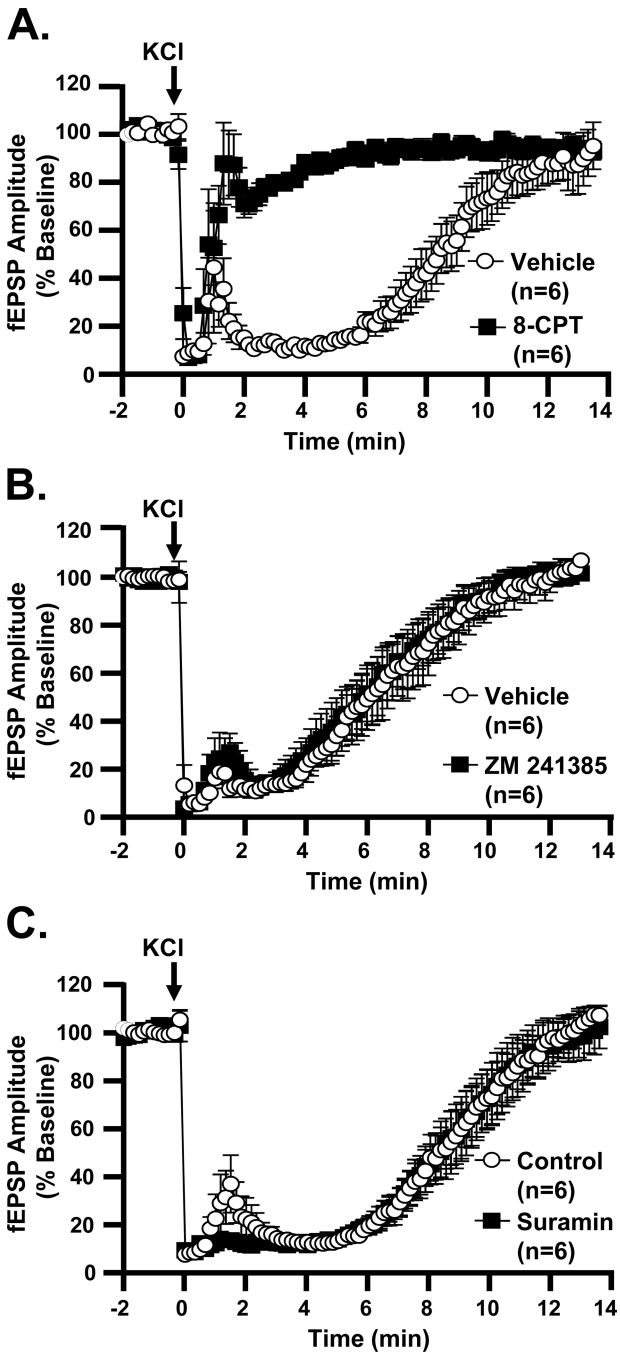

Figure 8. A1R antagonist, but not other purinergic receptor antagonists, abolishes secondary phase of synaptic depression after SD

A: The A1R antagonist 8-CPT (10 μM) accelerates recovery of fEPSPs after SD, by comparison with interleaved vehicle-treated slices (t_{50} 0.6±0.1 vs. 8.1±0.7 min, 8-CPT vs. vehicle, $p<0.0001$, unpaired t-test). **B:** Recovery of fEPSP amplitudes in the A2AR antagonist ZM 241385 (500 nM) closely matches that in vehicle (t_{50} 5.7±0.7 vs. 6.0±0.8 min, ZM 241385 vs. vehicle, $p=0.78$, unpaired t-test, n=6). **C:** Treatment with the P2R antagonist suramin (50 μM) does not change the time-course of fEPSP recovery (t_{50} 8.2±0.7 vs. 8.4±0.7 min, suramin vs. vehicle, $p=0.87$, unpaired t-test, n=6).

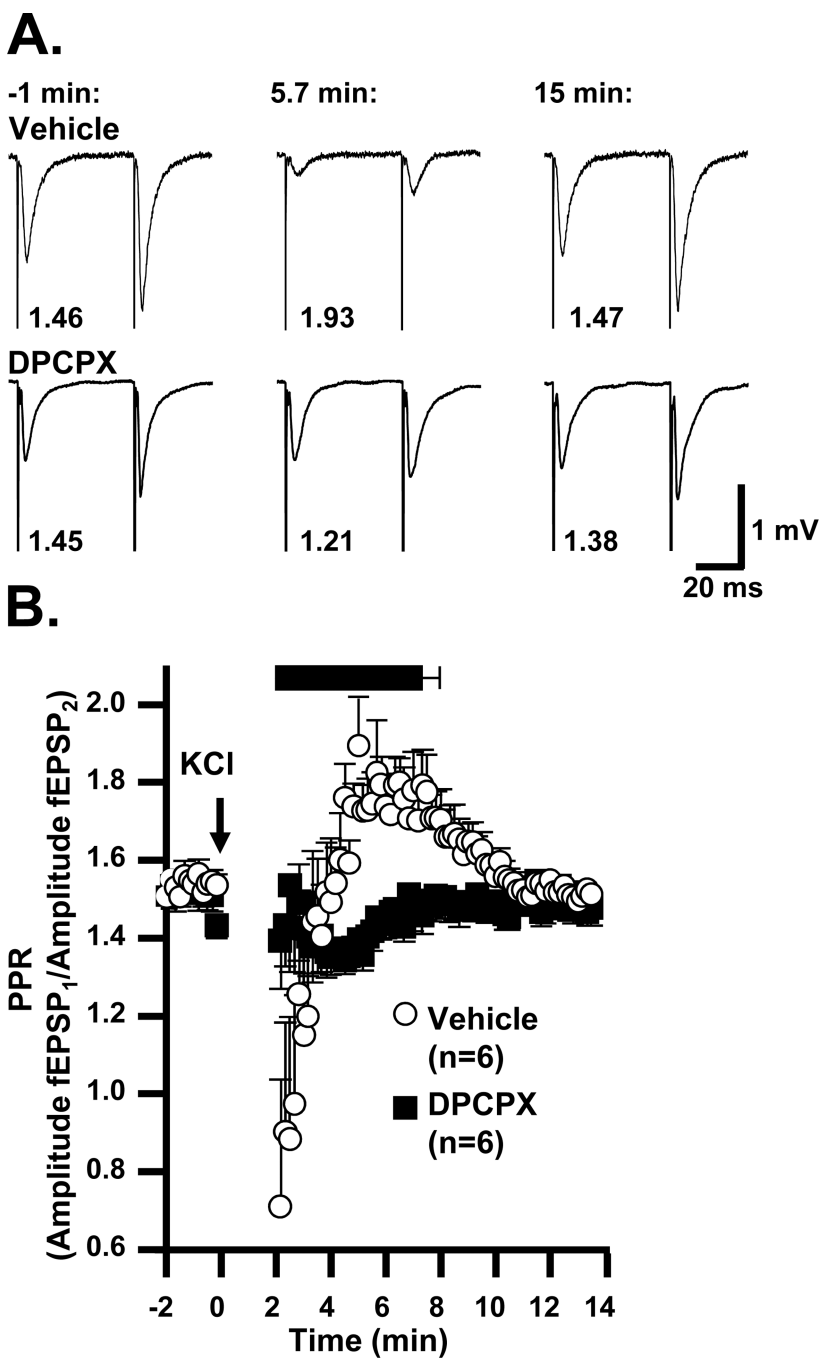

Figure 9. Adenosine A1 receptor activation during secondary synaptic depression is associated with increased paired pulse ratio (PPR)

A: Representative traces showing responses to pairs of stimuli (50 ms interstimulus interval), throughout SD. Times in minutes are relative to SD onset. Numbers under each stimulus pair are the calculated PPR (peak amplitude response 2 / response 1). **B:** Mean PPR values from interleaved vehicle (open circles) and DPCPX pre-exposed slices (500nM, filled squares). Two minutes of data (corresponding to the DC shift and immediate hyperexcitability) were omitted from analysis because fEPSP amplitudes were similar to baseline noise and/or were contaminated by population spikes. The black bar above the plot represents the mean±SEM period of secondary fEPSP suppression (> 50% baseline) vehicle-

treated slices. Note the period of elevated PPR (corresponding to decreased initial release probability) in the vehicle slices, which peaked during the period of secondary fEPSP suppression. DPCPX prevented this increase, and revealed a longer-lasting PPR decrease (increased initial release probability). PPR in vehicle was significantly higher than in DPCPX from 4.17 min to 8 min ($p<0.05$).